Imperfect Fabry-Perot resonators

Klaassen, T.

CHAPTER 7

Characterization of diamond-machined mirrors

Diamond-machining is used to fabricate the composite substrates elaborated on in Chapter 8 and 9. This technique causes a different type of irregularities than traditional grinding and polishing does. In this Chapter, the influence of the irregularities on the resonator dynamics will be investigated for a two-mirror cavity, where either one or both mirrors have been made by dielectric multi-layer coating of a diamond-machining produced substrate. Besides the tools discussed earlier in this Thesis, we also introduce polarization measurements to characterize the scattering.

7.1 Introduction

Precision machining dates back to World War 2, but substrates more or less acceptable for optical applications appeared only in the early 1970s [67]. State-of-the-art diamond-turned optics have a $\lambda/20$ peak-to-valley surface figure error and $0.2-0.4$ nm surface roughness [68]. Diamond-machining can be used to manufacture aspherical optics and offers the possibility to produce bifocal substrates, *i.e.*, substrates with a convex inner and a concave outer part, as used in Chapter 8 and 9. The convex inner part will also be denoted as "dimple". The surface of diamond-machined substrates shows periodic (circular) grooves due to the periodic movement of the diamond-chisel during machining. In this Chapter, we will investigate the effect of these grooves on the resonator dynamics of two conventional resonators, *i.e.*, without a dimple. The concave mirrors in the half-symmetric (flat/concave) and symmetric resonator (concave/concave) are, however, produced by diamond-machining, whereas the flat substrate is traditionally polished. The configurations in Chapter 8 and 9, comprising a bifocal mirror, are identical to the configurations investigated in this Chapter except for the central dimple inside the concave section.

This Chapter is organized as follows. The mirrors and setup are introduced in Section 7.2 and the mirror surface is interferometrically studied in Section 7.3. The cavity finesse and the losses deduced from the spectrum are discussed in Section 7.4. In Section 7.5, the influence of scattering on the polarization of the transmitted light will be demonstrated. We will end this Chapter with a conclusion.

7.2 Production of the mirrors

In an early stage of the project concerning the manufacturing of composite mirrors, we tried, in collaboration with Philips [69], to make the mirror substrates out of the polymers PMMA and Zeonex. The melting temperature, however, of both polymers is so low that the substrates deformed during the coating-procedure. Later, in collaboration with TNO [31], we moved to calcium fluoride (CaF_2) as the material out of which the substrates of our flat and concave mirrors have been made. Calcium fluoride is a crystal widely used for optical substrates, *e.g.*, in lithography systems, as it has a high transmission even at UV wavelengths as short as 175 nm [70]. The prime advantage of this material for our experiment is that it chips very fine during the diamond-machining procedure thus allowing for a low surface roughness. Furthermore, its melting temperature is very much higher than the temperature reached during the dielectric multi-layer coating process. This implies that the surface figure is maintained. Last but not least, CaF_2 is transparent at 800 nm. Drawbacks of CaF_2 are the low hardness and high coefficient of thermal expansion which make it less easy to work with than a standard substrate material as fused quarz.

The concave mirror is machined with a diamond chisel and has a radius of curvature $R = 14$ mm. The effective mirror diameter is $D = 2$ mm. For easy handling the substrates have a total diameter of 6 mm (see Fig. 7.1), of which the outer part is machined conically to prevent this part from scattering light back into the inner (concave) part via reflection by the other mirror of the cavity. For protection of the substrate, it is mounted in a metal ring. All substrates have been coated by LASEROPTIK [71] in the same coating run, with a stack of

24 layers of alternating Ta_2O_5 (refractive index 2.04) and SiO_2 (refractive index 1.46). The measured transmission of the coated flat substrate is $T = 8.3 \times 10^{-4}$ at 800 nm and assumed to be identical to the transmittance of other substrates coated in the same coating run. For accurate tuning of the cavity length, one mirror is placed on a translation stage (PI-M511). The resonator is scanned with a piezo (P-753.11C) to obtain a transmission spectrum. A lens ($f = 10$ cm) in front of the resonator mode-matches the input beam to the lowest-order mode of the cavity.

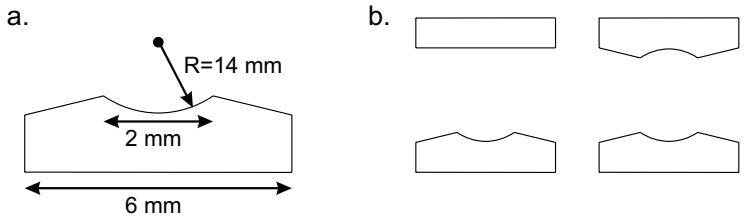

Figure 7.1: *(a) Sketch of the diamond-machined substrate, where the concave part is the actual mirror. The conical outer part prevents this part from reflecting light back into the inner part via reflection by the opposite mirror. (b) The half-symmetric and the symmetric cavity configuration.*

7.3 The mirror surface and scatter

The surface roughness of the bare substrate is measured with a WYKO interferometer at TNO [31] and found to be $\sigma \sim 2$ nm (RMS). We have to take into account that the roughness is measured over a limited area (100×100 μm^2), where the grooves are oriented predominantly in one direction. The total integrated scatter (TIS) and the surface roughness are related via TIS $= (4\pi\sigma/\lambda)^2$ [18]. Although this equation assumes randomly and not directionally distributed roughness, it gives a rough estimate of the TIS, being 1.0×10^{-3} in our case. Extra roughness introduced by the coating layers is neglected. From the measured transmittance and the calculated TIS we can calculate that the cavity finesse can be at most $F = \pi/(T + \text{TIS}) = 1500$.

The measurements with the WYKO interferometer do not only give us the surface roughness σ, but also the period of the grooves. The grooves formed by the diamond chisel resemble a somewhat irregular grating, having a period ranging from 10 to 25 μm. At a wavelength of 800 nm, such a period corresponds to scatter angles of $\alpha_s = 80 - 32$ mrad. Light scattered on the grooves will thus be displaced over $\Delta x = L\alpha_s = 0.4 - 0.16$ mm, per single-pass through a cavity length of $L = 5$ mm. Light scattered out of the lower-order modes can couple to higher-order modes with a 1D transverse mode number $m = (2\Delta x/w_0)^2 = 260 - 50$ [12], at a waist of $w_0 \sim 50$ μm. An alternative but equivalent calculation of the number of higher-order modes can be made in angular space. The beam angle of the fundamental mode in the far-field is $\alpha_0 = \lambda/(\pi w_0) = 5$ mrad [12]. Light scattered under an angle α_s can thus couple to modes with mode numbers $m = (\alpha_s/\alpha_0)^2 \approx 250 - 40$.

A first signature of scattering in our cavity is the appearance of Hercher fringes in the intensity profiles on the mirrors (Fig. 7.2a) close to frequency-degenerate points. Although

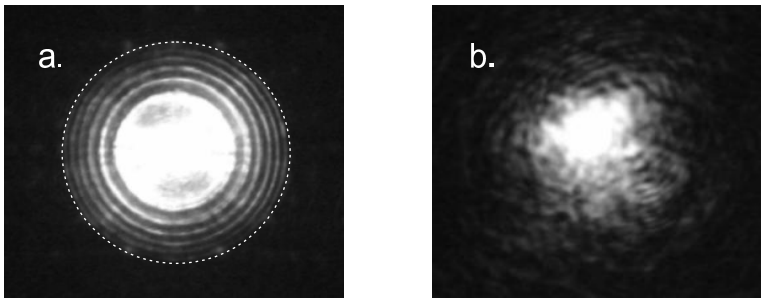

Figure 7.2: *(a) Image made with an imaging lens behind the cavity of Hercher fringes in the symmetric configuration close to a 4-fold frequency-degenerate cavity length ($\Delta L = 60\ \mu m$). The outer fringe (dashed circle) coincides with the radius (1 mm) of the mirror. (b) Intensity profile of a distorted TEM_{00} observed at a fixed cavity length close to 4-fold frequency-degenerate cavity length ($\Delta L = 100\ \mu m$).*

we inject only on-axis, fringes appear over the full mirror-aperture due to resonant trapping of scattered light (also see Chapter 4). A second signature of scattering is the mode coupling observed in the transmitted intensity profile of an injected TEM_{00}-mode as shown in Fig. 7.2b. The profile of the transmitted eigenmode is not a nice Gaussian TEM_{00}, but also shows the admixture of higher-order Gaussian modes (see Chapter 3). The cavity length is fixed to the resonance of the TEM_{00}-mode by manually tuning the piezo-voltage.

7.4 Spectra and imperfections

Typical transmission spectra of the symmetric and half-symmetric cavities are shown in Fig. 7.3, where the TEM_{00}-like mode is excited predominantly. Both spectra are stable over time and look similar to spectra from resonators using mirrors based upon traditionally polished substrates.

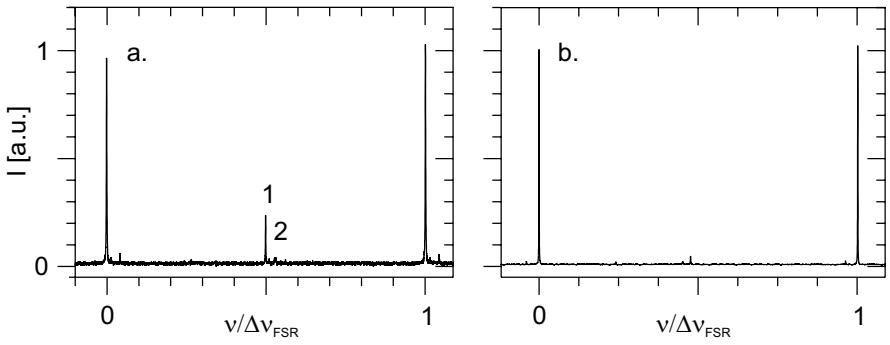

Figure 7.3: *Transmission spectra slightly away from $N = 4$ of (a) a half-symmetric ($L \approx 7.0$ mm) and (b) a symmetric resonator ($L \approx 4.1$ mm)*

We measured the finesse several times, after taking out one of the mirrors and realigning the cavity every attempt. The highest measured finesse is $F = 1280 \pm 50$. This experimental finesse is in the order of the finesse estimated from the surface roughness. Using $F = \pi/(A + T)$ and $T = 8.4 \times 10^{-4}$ we calculate a loss $A = 1.6 \times 10^{-3}$, to be compared with the estimate of TIS$= 1.0 \times 10^{-3}$ as given above. This means that only $8.4 \times 10^{-4}/2.44 \times 10^{-3} \times 100\% \sim$ 34 % of the light leaves the resonator via the mirrors, while the other 66 % is scattered away. From these numbers, we expect a peak transmission for the lowest order mode of $\eta^2 = [T/(A+T)]^2 = 12$ %, which agrees approximately with our experimental observation of $\eta^2 = 9$ %. This means that we are able to mode-match very well and inject most of the light into the TEM_{00}-mode.

An important experimental observation is that the resonance width and peak transmission depend strongly on both the alignment and the length detuning. Tilting the back-mirror over $\sim 0.1^\circ$ can change the peak transmission by as much as a factor 10, and a length detuning of only $\Delta L \sim 0.6$ μm can already change the peak transmission η^2 by (relatively) 30 %. Although the loss increases in both cases, we are always able to predominantly excite the TEM_{00}-mode. The sensitivity to angular alignment can be easily understood as the waist of the fundamental mode on the mirror ($w_0 = 50$ μm for $L = 5$ mm) is just a few times bigger than the period of the grooves ($10 - 25$ μm) on the mirrors. The sensitivity to a length detuning over only $\Delta L \sim 0.6$ μm is very surprising, and not yet understood.

At degeneracy $N = 4$ and on-axis injection, the odd modes in the spectrum with ditto summed transverse mode numbers $m+n$ at $\nu/\Delta\nu_{\mathrm{FSR}} \sim 0.25$ and 0.75 are not excited due to proper (inversion-symmetric) alignment. Some even modes, other than the TEM_{00} remain, however, *e.g.*, the two tiny modes (denoted 1 and 2) at $\nu/\Delta\nu_{\mathrm{FSR}} \sim 0.5$. From manual tuning of the piezo-amplifier we can identify these modes with a camera behind the resonator as the TEM_{02} and TEM_{20}.

The lifted degeneracy of these modes allows us to quantify the astigmatism as one of the aberrations of the cavity. The measured spectral spacing $\Delta\nu/\Delta\nu_{\mathrm{FSR}} \sim 2\%$ can be converted into the deviation of the mirror radius ΔR compared to the average radius of curvature R. Substitution of 0.50 and 0.52 for $n+m = 2$ in $(\nu_{nm} - \nu_{00})/\Delta\nu_{\mathrm{FSR}} = (n+m)\theta_0/2\pi = (n+m)\arccos(\sqrt{1-L/R})/\pi$ results in $\Delta R/R \sim 6$ %. This large value is likely to represent the relative difference in the "local curvature" on the probed mirror surface. A similar argument has been given to explain the observed astigmatism in "super-cavities" [56].

The mode coupling, mentioned earlier in relation to the mode profile, appears also in the spectra. Taking a closer look at the dominant resonances (not shown in detail here) we observe weakly excited higher-order modes that couple with the TEM_{00}-mode. Consequently, the lineshape of the resonances in the spectrum is not fully Lorentzian and the width and height vary close to frequency-degeneracy. As the lineshape of the resonances is distorted by mode coupling, it would have been better to determine the cavity finesse by a cavity ring-down experiment. This is, however, not a trivial experiment as the $1/e$-decay time is very short; we expect roughly $\tau = FL/(\pi c) \sim 0.1$ ns.

7.5 Polarization and scattering

In this last Section, we study the polarization of the light transmitted through a cavity, comprising again a flat and a concave mirror, but now with a polarizer behind the resonator. We inject vertically polarized light off-axis at an angle, as compared to the optical axis, in the 8-fold frequency-degenerate cavity ($L = 2$ mm). For a transmission axis of the polarizer parallel to the input polarization we clearly observe 8 hit points on the mirror as shown in Fig. 7.4a. When we rotate the polarizer over 90°, we still observe the hit points on the mirror as shown in Fig. 7.4b. This is surprising as intuitively one would expect that the polarization should be preserved inside the resonator, and the component perpendicular to the input polarization would be zero. In practice, the light behind the cavity contains, however, a surprisingly large component with a polarization perpendicular to the input polarization. More specifically, the intensity in the hit points is only 75× weaker for polarization perpendicular to the input polarization than for the parallel component. This observation is not an artifact of our polarizer. Our Polarcor^{TM} polarizer (Newport 05P109AR.16) is well-suited for this experiment: it has a specified acceptance angle as large as 15° (typical angles for our configuration are 2°) and the combination of the laser and the polarizer has a measured extinction ratio of 35000 : 1 for normal incidence.

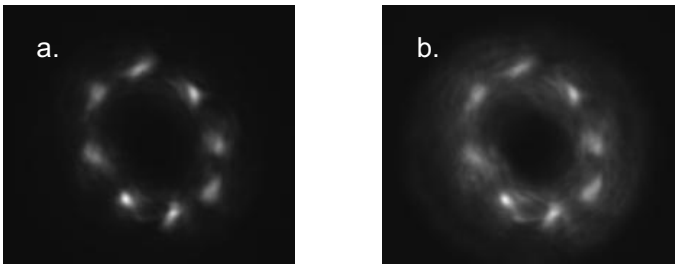

Figure 7.4: *Intensity profiles of a corkscrew-like ring mode on the mirror of a cavity comprising a flat and a concave mirror. The 8 hit points on the mirror show the 8-fold frequency-degeneracy of the resonator at a cavity length of $L = 2$ mm. The circle described by the hit points has a diameter of* 0.46 *mm. The transmission axis of the polarizer behind the cavity is (a) parallel and (b) perpendicular to the input polarization. The shutter time of the camera is much bigger than the scan duration through a free spectral range:* $0.5\ s > 0.05\ s$.

The observation discussed above might be related to other physics than scattering. The measured depolarization could result from a geometrical (or Berry) phase [72, 73], that quantifies the polarization rotation experienced by orbits that do not propagate in a single plane.

Taking a closer look at the intensity profiles, we observe furthermore that the intensity profile for perpendicular polarization has a relatively brighter "circular background". The origin of the light inbetween the hit points lies in the fact that light is scattered out of the hit points by surface roughness of the mirrors. This scattering-induced depolarization of the light has a different origin than the geometrical depolarization mentioned before and is reflected in the different ratios for the intensities in the hit points and the average throughput.

Cross-sections of the intensity profiles, show that the maximum intensity of the background normalized to the intensity in the hit points is 0.25 and 0.10 for perpendicular and parallel polarization, respectively. This means that for parallel polarization the light is more confined in the hit points, whereas for perpendicular polarization the light is spread more equally over the mirror.

7.6 Conclusion

We have demonstrated that a cavity comprising diamond-machined mirrors can achieve a finesse of $F = 1300$, comparable to the finesse ($F = 1 \times 10^3 - 1 \times 10^4$) achieved in standard Fabry-Perot resonators (dimensions ~ 1 cm and standard coating procedure). The alignment of a diamond-machined cavity is, however, more subtle due to the periodic grooves in the substrates made by the diamond chisel.